

Multiple-Decker Sandwich Complexes of Lanthanide–1,3,5,7-Cyclooctatetraene [Ln_n(C₈H₈)_m] (Ln = Ce, Nd, Eu, Ho, and Yb); Localized Ionic Bonding Structure

Tsuyoshi Kurikawa, Yuichi Negishi, Fumitaka Hayakawa, Satoshi Nagao, Ken Miyajima, Atsushi Nakajima, and Koji Kaya*

Contribution from the Department of Chemistry, Faculty of Science and Technology, Keio University, 3-14-1 Hiyoshi, Kohoku-ku, Yokohama 223-8522, Japan

Received July 10, 1998

Abstract: Organometallic lanthanide complexes of Ln_n(C₈H₈)_m (Ln = lanthanide metals of Ce, Nd, Eu, Ho, and Yb; C₈H₈ = 1,3,5,7-cyclooctatetraene) were produced by a combination of laser vaporization and molecular beam methods. The complexes having (n, m) = (n, n + 1) for n = 1–5 were prominently produced as magic numbers in the mass spectra. Using mass spectrometry, photoionization spectroscopy, and photoelectron spectroscopy, it is concluded that these magic-numbered complexes form multiple decker sandwich structures in which Ln atoms and C₈H₈ molecules are alternately piled up. The obtained spectroscopic data show that these sandwich complexes are formed through ionic bonds and are charge transfer complexes, where the Ln atoms are multiply charged cations of Ln^{k+} (k = 2 and 3) and C₈H₈ molecules are multiply charged anions.

1. Introduction

The f-block elements of lanthanide (Ln) and actinide (Ac) metals have been of considerable importance in many areas of modern technology.^{1–4} After discovery of Ac(C₈H₈)₂,^{5–7} studies on this criteria have extensively stimulated experimentalists and theoreticians, since these complexes showed highly symmetric D_{8h} compounds in which 4-fold positive central metal ions of Ac⁴⁺ are sandwiched by two aromatic eight-membered rings of C₈H₈²⁻. A certain amount of 5f(Ac)–π(C₈H₈) overlap was suggested, which led to a conclusion of dominant character of covalency in this system.^{8–10} On the other hand, Ln(C₈H₈)₂ complexes were proved to take trivalent complexes in bulk materials^{3,11} and in theoretical calculations,^{12–14} except for divalent complexes of Ln = Eu and Yb. Lanthanide π-carbocyclic complexes were synthesized as their salts of K[Ln(C₈H₈)₂] by Hodgson et al.,^{9,11} where trivalency of Ln metals overcomes aromaticity of C₈H₈²⁻, resulting in a complex

denoted as Ln³⁺(C₈H₈^{1.5-})₂. An ionic character well describes these phenomena rather than the covalent one, where little overlap of 4f(Ln) and π(C₈H₈) electrons exists and directional bonding is relatively unimportant. This predominantly ionic character results from which C₈H₈ ligand can act as a stable dianion, as is well-known in the related actinide compounds. In the condensed phase, therefore, the alkali metal salts of M_{alkali}⁺[Ln³⁺(C₈H₈²⁻)₂] are generally prepared, where positively charged M_{alkali}⁺ compensates the discrepancy between 3+ oxidation states of Ln atoms and the negative charge of 4– from two C₈H₈ ligands. Among 14 lanthanide elements, there are 2+ oxidation state complexes of Eu and Yb that form in bulk as (M_{alkali}⁺)₂[Ln²⁺(C₈H₈²⁻)₂].^{15–17}

These properties of Ln metals indeed retard studies on neutral and multicore complexes of Ln_n(C₈H₈)_m. Until now, only two synthetic studies on Ce₂(C₈H₈)₃¹⁸ and [(C₈H₈)Nd(THF)₂][(C₈H₈)₂-Nd]¹⁹ have been reported. In the divalent Ln(C₈H₈) (Ln = Eu and Yb),^{20,21} the half-sandwich complexes with solvent molecule seem to preclude intrinsic growth. Thus, due to unfavored solvation, detailed study on the Ln–C₈H₈ system has been delayed.

The application of the laser vaporization to the gas-phase synthesis of organometallic compounds enables us to prepare the constituents in considerable density in a short time because there are no interfering effects of solvents, aggregation phe-

* Address correspondence to this author.

(1) Marks, T. J. *Prog. Inorg. Chem.* **1978**, *24*, 51.

(2) Green, J. C. *Struct. Bonding (Berlin)* **1981**, *43*, 64.

(3) Schumann, H.; Meese-Marktscheffel, J. A.; Esser, L. *Chem. Rev.* **1995**, *95*, 865.

(4) Marks, T. J.; Ernst, R. D. *Compr. Organomet. Chem.* **1982**, *3*, 192.

(5) Streitwieser, A., Jr.; Müller-Westerhoff, U. *J. Am. Chem. Soc.* **1968**, *90*, 7364.

(6) Zalkin, A.; Raymond, K. N. *J. Am. Chem. Soc.* **1969**, *91*, 5667.

(7) Streitwieser, A., Jr.; Yoshida, N. *J. Am. Chem. Soc.* **1969**, *91*, 7528.

(8) Karraker, D. G.; Stone, J. A.; Jones, E. R., Jr.; Edelstein, N. *J. Am. Chem. Soc.* **1970**, *92*, 4841.

(9) Streitwieser, A., Jr.; Müller-Westerhoff, U.; Sonnichsen, G.; Mares, F.; Morrell, D. G.; Hodgson, K. O.; Harmon, C. A. *J. Am. Chem. Soc.* **1973**, *95*, 8644.

(10) Raymond, K. N.; Eigenbrot, C. W., Jr. *Acc. Chem. Res.* **1980**, *13*, 276.

(11) Hodgson, K. O.; Raymond, K. N. *Inorg. Chem.* **1972**, *11*, 3030.

(12) Dolg, M.; Fulde, P.; Küchle, W.; Neumann, C.; Stoll, H. *J. Chem. Phys.* **1991**, *94*, 3011.

(13) Dolg, M.; Fulde, P.; Stoll, H.; Preuss, H.; Chang, A.; Pitzer, R. M. *Chem. Phys.* **1995**, *195*, 71.

(14) Liu, W.; Dolg, M.; Fulde, P. *J. Chem. Phys.* **1997**, *107*, 3584.

(15) Kinsley, S. A.; Streitwieser, A., Jr.; Zalkin, A. *Organometallics* **1985**, *4*, 52.

(16) Kinsley, S. A.; Streitwieser, A., Jr.; Zalkin, A. *Acta Crystallogr.* **1986**, *C42*, 1092.

(17) Evans, W. J.; Shreeve, J. L.; Ziller, J. W. *Polyhedron* **1995**, *14*, 2945.

(18) Greco, A.; Cesca, S.; Bertolini, G. *J. Organomet. Chem.* **1976**, *113*, 321.

(19) (a) DeKock, C. W.; Ely, S. R.; Hopkins, T. E.; Brault, M. A. *Inorg. Chem.* **1978**, *17*, 625. (b) Ely, S. R.; Hopkins, T. E.; DeKock, C. W. *J. Am. Chem. Soc.* **1976**, *98*, 1624.

(20) Hayes, R. G.; Thomas, J. L. *J. Am. Chem. Soc.* **1969**, *91*, 6876.

(21) Wayda, A. L.; Mukerji, I.; Dye, J. L.; Rogers, R. D. *Organometallics* **1987**, *6*, 1328.

nomena, and counterions. This new approach should open up an area of organometallic chemistry and physics that can be studied quite nicely in the gas phase. The object of this work is to investigate the nature of multicore complexes from the spectroscopic point of view and to elucidate their electronic structures. In the present paper, we will give experimental results on the gas-phase preparation of the multiple-decker sandwich clusters of $\text{Ln}_n(\text{C}_8\text{H}_8)_{n+1}$ for five Ln metals of Ce, Nd, Eu, Ho, and Yb that are representative of multivalent ions such as $\text{Ce}^{3+(4+)}$, Nd^{3+} , Eu^{2+} , Ho^{3+} , and Yb^{2+} , respectively. The electronic structure and bonding are discussed based on the results of the photoelectron spectroscopy of $\text{Ln}(\text{C}_8\text{H}_8)_2^-$ anion and ionization energy (E_i) of the neutral $\text{Ln}_n(\text{C}_8\text{H}_8)_{n+1}$ clusters. The photoelectron spectra and size dependence of E_i can reveal the ionic bonding nature including the oxidation states. The localized charge distribution on both Ln atoms and C_8H_8 ligands governs the electronic features of the complexes, and the multiply charged Ln^{k+} atoms isolated by the ligands implies the new possibility of the optical material and the electron spin chemistry. The electronic properties of the Ln- C_8H_8 will be discussed in comparison with those of the sandwich complexes between transition metal atoms and benzene molecules,²² which have delocalized electronic structure along the molecular axis.

2. Experimental Section

Lanthanide-cyclooctatetraene complexes, $\text{Ln}_n(\text{C}_8\text{H}_8)_m$ [Ln = lanthanide metals of Ce, Nd, Eu, Ho, and Yb; C_8H_8 = 1,3,5,7-cyclooctatetraene], were produced by a combination of the laser-vaporization method, a molecular beam method, and a flow tube reactor (FTR). An experimental setup used in this work is described elsewhere.^{22–24} First, Ln atoms were vaporized by the frequency doubled output from a Q-switched Nd^{3+} :YAG laser (532 nm, ~ 10 mJ/pulse). Then the vaporized atoms were cooled by a He carrier gas (5 atm stagnation pressure) in a growth channel (3 mm diameter and 4 cm length) and were synchronously mixed with the C_8H_8 vapor pulse (~ 70 Torr; 70 °C) diluted with 1.5 atm of He carrier gas at FTR. $\text{Ln}_n(\text{C}_8\text{H}_8)_m$ binary complexes thus generated were sent into the ionization chamber through a skimmer (3 mm diameter). Then the complexes were ionized by an ArF excimer laser (193 nm; 6.42 eV) or a frequency doubled output of a tunable dye laser pumped by a XeCl excimer laser (308 nm; 4.03 eV) in a static electric field. The photoions were mass-analyzed by a reflectron time-of-flight (RETOF) mass spectrometer. To get information on the structures of the complexes, $\text{Ln}_n(\text{C}_8\text{H}_8)_m$ were further reacted with CCl_4 gas diluted with 1.5 atm of He inside the second FTR, which was mounted downstream of the C_8H_8 addition port. To determine ionization energies (E_i s), the frequency doubled output of the dye laser was used as the ionization laser. Photon energy was changed at a 0.01–0.05 eV interval in the range of 5.92–3.90 eV, while the abundance and composition of $\text{Ln}_n(\text{C}_8\text{H}_8)_m$ were monitored by the ionization of the ArF laser. Fluences of both the dye laser and the ArF laser were monitored by a pyroelectric detector (Molelectron J-3) and were kept at $\sim 200 \mu\text{J}/\text{cm}^2$ to avoid multiphoton processes. To obtain photoionization efficiency (PIE) curves, ion intensities of the mass spectra were plotted as a function of photon energy with normalization to both the laser fluence and the ion intensities of the ArF mass spectra. E_i s of $\text{Ln}_n(\text{C}_8\text{H}_8)_m$ were determined from the final decline of the PIE curves. The typical uncertainty of E_i s is estimated to be ± 0.05 eV.

To record photoelectron spectra, anionic complexes produced by the above procedure were sent into an on-line TOF mass spectrometer to

3 keV for mass analysis and 900 eV for PES (photoelectron spectroscopy) study. After being decelerated, the mass-selected anions were photodetached with the third harmonic (355 nm, 3.49 eV) or the fourth harmonic (266 nm, 4.66 eV) of the other Nd^{3+} :YAG laser. The photoelectron signal was typically accumulated to 30 000 shots by a multichannel scaler/averager (Stanford Research System, SR430). Obtained energy resolution was about 70 meV fwhm at 1 eV electron energy. The energy of the photoelectron was calibrated by measuring photoelectron spectra of Au^- . The laser power for photodetachment was in the range of 10–20 mJ/cm² for 355 nm and 1–3 mJ/cm² for 266 nm, and no power dependent processes for the spectrum shape were observed.

3. Results and Discussion

3.1. Mass Spectra of $\text{Ln}_n(\text{C}_8\text{H}_8)_m$ Complexes. Figure 1a–e show typical examples of the photoionization mass spectra of $\text{Ln}_n(\text{C}_8\text{H}_8)_m$ [Ln = lanthanide metals of Ce, Nd, Eu, Ho, and Yb; henceforth (n, m)] produced by the foregoing procedure. To enhance the ion intensity of larger complexes, the transmission efficiency of the mass spectrometer was optimized around 1000–1500 u with a pair of deflection plates. Main peaks in each spectrum except for Ce showed almost the same compositions denoted as ($n, n + 1$). Even when the concentration of C_8H_8 vapor was increased, these main peaks remained unchanged in the mass spectra. Therefore, these ($n, n + 1$) species are indeed abundant and stable complexes formed in the saturated high concentration of C_8H_8 . In case of Ce, ($n, n + 1$) series were not necessarily observed as magic numbers, because vaporized Ce itself easily reacts with contamination of O_2 and H_2O in the He carrier gas. Although the ion intensity was relatively low compared to other lanthanide elements, $\text{Ce}_n(\text{C}_8\text{H}_8)_m$ are mainly produced also at ($n, n + 1$).

The regular pattern in the mass spectra implies that these complexes consist of accumulation of a certain unit. The most probable structure is a multiple-decker sandwich structure by analogy to the structure of the transition metal–benzene complexes,^{22,25} in which transition metal atoms and benzene molecules are alternately piled up (Figure 2). As discussed later in the following sections, the characteristic electronic structures can be explained by the sandwich structures. In fact, it is natural to extend the single sandwich structure into the multiple sandwich one, because the triple-decker structure of Ce– C_8H_8 or Nd– C_8H_8 was synthesized in the condensed phase.^{18,19} Since the advantage of the gas-phase synthesis is no environmental factors such as organic solvents, it seems that these novel structures can possibly be synthesized.

3.2. Photoelectron Spectroscopy of $\text{Ln}(\text{C}_8\text{H}_8)_2^-$ (Ln = Ce, Nd, Eu, Ho, and Yb) Anions. To elucidate the further bonding nature of these complexes, we conducted PES experiments of the anions, $\text{Ln}(\text{C}_8\text{H}_8)_2^-$, at 266 (4.66 eV) and 355 nm (3.49 eV) (Figure 3). In the formation of Ln– C_8H_8 anions, larger complexes of ($n, n + 1$)[−] at $n \geq 2$ could be produced only for Eu and Yb, while (1, 2)[−] was mainly produced for Ce, Nd, and Ho. This feature can be explained by the electronic structure, which will be discussed later.

In the PES spectra, the horizontal axis corresponds to an electron-binding energy, E_b , which is defined as $E_b = h\nu - E_k$, where E_k is a kinetic energy of the photoelectron and $h\nu$ is a photon energy of the photodetachment laser. To assign a photodetachment threshold energy, E_T , the slope of the first onset was extrapolated linearly to the baseline of the spectrum. A downward arrow indicates the E_T value in each figure. The

(22) Hoshino, K.; Kurikawa, T.; Takeda, H.; Nakajima, A.; Kaya, K. *J. Phys. Chem.* **1995**, *99*, 3053.

(23) Kurikawa, T.; Hirano, M.; Takeda, H.; Yagi, K.; Hoshino, K.; Nakajima, A.; Kaya, K. *J. Phys. Chem.* **1995**, *99*, 16248. Kurikawa, T.; Takeda, H.; Nakajima, A.; Kaya, K. *Z. Phys. D* **1997**, *40*, 65.

(24) Nagao, S.; Kurikawa, T.; Miyajima, K.; Nakajima, A.; Kaya, K. *J. Phys. Chem. A* **1998**, *102*, 4495.

(25) Weis, P.; Kemper, P. R.; Bowers, M. T. *J. Phys. Chem. A* **1997**, *101*, 8207.

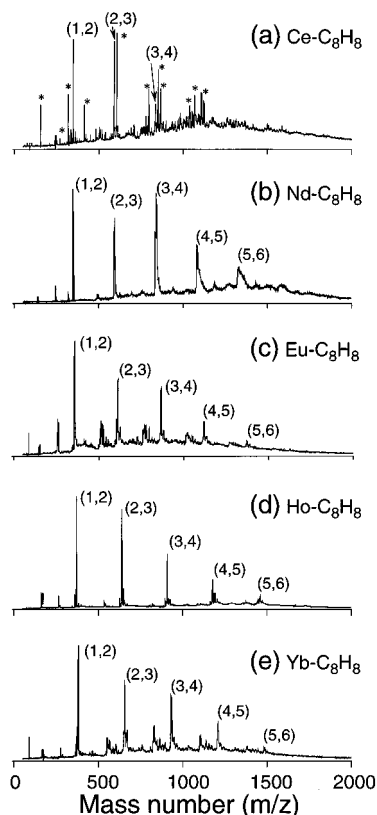


Figure 1. Time-of-flight mass spectra of lanthanide (Ln)–1,3,5,7-cyclooctatetraene (C_8H_8) complexes, $Ln_n(C_8H_8)_m$ [Ln = Ce (a), Nd (b), Eu (c), Ho (d), and Yb (e)] obtained by the photoionization of the ArF laser (6.42 eV). Peaks are labeled according to the notations (n, m), denoting the number of Ln atoms (n) and C_8H_8 molecules (m). Only for Ce are oxide or hydroxide prominent (marked with asterisk) due to high reactivity of Ce. For Nd– C_8H_8 , mass peaks become broader with increasing mass due to many isotopes of Nd atoms.

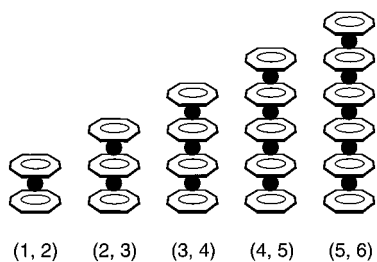


Figure 2. Proposed structures of $Ln_n(C_8H_8)_{n+1}$ complexes ($n = 1-5$).

E_T values correspond to upper limits of the adiabatic E_{AS} . Besides the E_T values, vertical detachment energies (VDEs) of the first peak are also derived from the peak maxima in the photoelectron spectra. VDEs are energies of maximum overlap between the nuclear wave functions of the ground state between anions and neutrals. E_T s and VDEs are tabulated in Table 1, including VDEs of successive peak(s). The successive peaks correspond to the photodetachment into the vibrationally or electronically excited states of the corresponding neutral.

At first glance of the five photoelectron spectra, a striking similarity is readily recognized and they are classified into two groups: one is $Ce(C_8H_8)_2^-$, $Nd(C_8H_8)_2^-$, and $Ho(C_8H_8)_2^-$ and the other is $Eu(C_8H_8)_2^-$ and $Yb(C_8H_8)_2^-$. In the former group, two peaks are located around the binding energy of 2.5 and 3.5 eV, and they have similar profiles with a sharp leading edge and a couple of shoulders on the higher binding energy side. In the latter group, the first two sharp peaks are located around 2.0 and 2.5 eV, and they are accompanied by a weaker broad

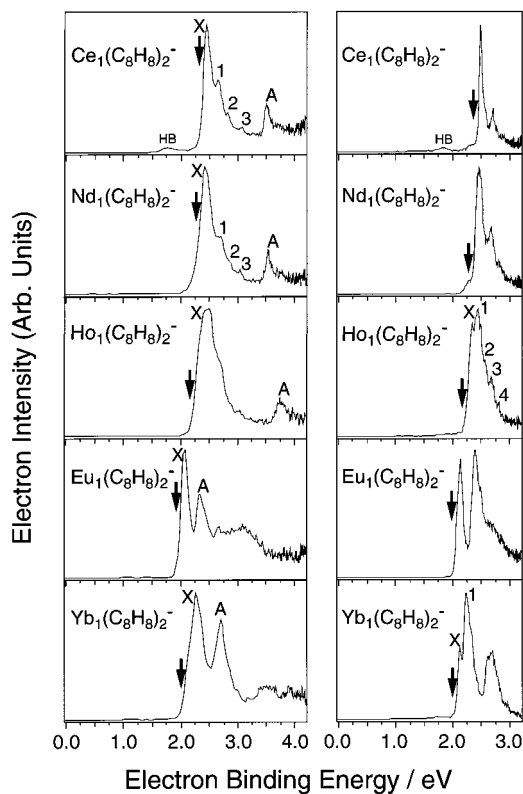


Figure 3. Photoelectron spectra of $Ln(C_8H_8)_2^-$ anions (Ln = Ce, Nd, Eu, Ho, and Yb) at 266 nm (4.66 eV) for the left side and 355 nm (3.49 eV) for the right side. Arrows indicate threshold energies (E_T). The vertical detachment energy of each labeled peak is tabulated in Table 1. Peaks labeled “HB” refer to hot bands.

Table 1. Threshold Energies (E_T s) and Vertical Detachment Energies (VDEs) of $Ln(C_8H_8)_2^-$ (eV)^a

Ln	E_T		VDE
Ce	2.42(32)	X	2.45
		1	2.66
		2	2.84
		3	3.09
		A	3.51
Nd	2.37(25)	X	2.43
		1	2.72
		2	2.81
		3	3.09
		A	3.54
Eu	2.02(09)	X	2.14
		A	2.68
Ho	2.18(18)	X	2.34
		1	2.45
		2	2.57
		3	2.66
		4	2.82
		A	3.75
Yb	1.95(10)	X	2.13
		1	2.24
		A	2.65

^a Numbers in parentheses indicate experimental uncertainties; 2.42(32) represents 2.42 ± 0.32 .

band in the higher binding energy. The similarity in these two groups is ascribed to a common electronic feature; they are characterized as a highly ionic complex that depends not on the metal elements, but on the oxidation state. It is reasonable to assume that Ce, Nd, and Ho all take the oxidation state of +3, while both Eu and Yb take that of +2, by analogy to the reported lanthanide complexes.^{3,11-17}

3.2.a. Photoelectron Spectra of Ce(C₈H₈)₂, Nd(C₈H₈)₂, and Ho(C₈H₈)₂. As is well-known by the $4n + 2$ rule of aromatics, a C₈H₈ molecule can act as an electron acceptor of two electrons, because (1) the LUMO nearly degenerated with the HOMO accepts two electrons and (2) the two excess electrons complete the aromaticity of the eight-membered ring in the C₈H₈ molecule.²⁶ In fact, Ce(C₈H₈)₂, Nd(C₈H₈)₂, and Ho(C₈H₈)₂ in bulk materials have been prepared as potassium or lithium salts denoted as M_{alkali}⁺[Ln³⁺(C₈H₈)₂]^{3,11} and then it is rational to consider that the anions of [Ln(C₈H₈)₂]⁻ can be expressed as a Ln³⁺(C₈H₈)₂⁻ configuration for Ce, Nd, and Ho. On the configuration, each C₈H₈ molecule has two excess electrons. Namely, the (1, 2)⁻ should become stable with the electronic demands of Ln³⁺ and C₈H₈²⁻. As discussed before, the anions of (1, 2)⁻ were mainly produced for Ce, Nd, and Ho in the mass spectra, which should be attributed to the ionic electronic structure of the charge balance in (1, 2)⁻.

In the oxidation states of 3+, Ce³⁺, Nd³⁺, and Ho³⁺ have 1, 3, and 10 f electron(s), respectively. As shown in their photoelectron spectra, this difference does not change the spectra. This is because the bands in the spectra come predominantly from the molecular orbital of the ligand molecules. By analogy to the photoelectron spectra of cerocene, uranocene, and thorocene, the bands of X and A are undoubtedly associated with electron detachment from the e_{2u} and e_{2g} molecular orbitals, respectively.^{27,28} The fine structures associated with the band X are probably due to vibrations of the C₈H₈ ligands in the neutral lanthanocene.

Streitwieser et al.²⁷ proposed in a PES experiment for neutral Ce(C₈H₈)₂ that the configuration of its neutral ground state is (a_{1g}; 2C₈H₈)²(a_{2u}; 2C₈H₈)²(e_{1g}; 2C₈H₈)⁴(e_{1u}; 2C₈H₈)⁴(e_{2g}; 2C₈H₈)⁴-(e_{2u}; 2C₈H₈)³(e_{3u}; Ce)¹, and that the energy difference between e_{2u} and e_{2g} is about 0.93 eV. Since the ground-state configuration of neutral Ln⁴⁺(C₈H₈)₂ is unlikely from several theoretical calculations,¹²⁻¹⁴ we determined that the configurations for the anion and the neutral in the case of Ce are Ln³⁺(C₈H₈)₂⁻ [(e_{2g}; 2C₈H₈)⁴(e_{2u}; 2C₈H₈)⁴(e_{3u}; Ln)¹] and Ln³⁺(C₈H₈)₂^{1.5-} [(e_{2g}; 2C₈H₈)⁴(e_{2u}; 2C₈H₈)³(e_{3u}; Ln)¹], respectively. Then, the plausible assignment is that the first peak of X corresponds to the photodetachment from the e_{2u} MO of C₈H₈ and the second peak of A corresponds to that from the e_{2g} MO of C₈H₈, assuming D_{8h} symmetry. For Ln = Ce, Nd, and Ho, the anions of Ln(C₈H₈)₂⁻ are reasonably assumed to have D_{8h} symmetry in the gas phase, because the C₈H₈ ligands become C₈H₈²⁻ with Ln³⁺. Since C₈H₈²⁻ satisfies the aromaticity of $4n + 2$ due to the 10-electron system, the ligand becomes planar.²⁶ Indeed, the symmetry of D_{8h} has been found by crystal studies for alkali metal salts of M_{alkali}[Ln(C₈H₈)₂]¹⁻⁴ Under the representations of the D_{8h} point group, the most important covalent contributions to metal-ring bonding may arise from metal 5d(e_{2g}) and 4f(e_{2u}) orbitals interacting with the high-lying π orbitals (e_{2u}, e_{2g}) of the C₈H₈ ligands. For cerocene⁺ produced by the photoionization of cerocene, it was reported that the energy gap between e_{2u} and e_{2g} MOs is 0.93 eV.²⁷ As listed in Table 1, on the other hand, the gaps are 1.06, 1.11, and 1.41 eV²⁹ for the neutral Ce(C₈H₈)₂, Nd(C₈H₈)₂, and Ho(C₈H₈)₂. The larger gap of the neutral cerocene compared to that of cerocene⁺

should be attributed to the stronger ionic interaction; Ce³⁺ interacts with two C₈H₈^{1.5-} in the neutral, whereas Ce³⁺ interacts with two C₈H₈¹⁻ in the cation.

Peaks from 1 to 3 in Ce and Nd can tentatively be assigned as the C=C symmetric stretching mode (1651 cm⁻¹; 0.205 eV)³⁰ accompanied by structural deformation from C₈H₈²⁻ to C₈H₈^{1.5-}, although peaks from 1 to 4 in Ho(C₈H₈)₂ differ from Ce and Nd cases. From Ce(C₈H₈)₂⁻ to Ho(C₈H₈)₂⁻, the apparent broadening of these bands with the heavier lanthanide atoms is noticeable, which is attributed to the exchange interaction with the unpaired f electrons. As discussed by Liu et al.,¹⁴ the ground states for the lighter and heavier lanthanocenes are respectively the lower and higher multiplicity states resulting from the coupling between the central metal 4fⁿ subshell and the unpaired electron of the π ligand. It was theoretically suggested^{12,13} that cerocene, Ce(C₈H₈)₂, is a Ce(III) compound, in which a Ce³⁺ ion having a 4f¹ configuration is sandwiched by two C₈H₈^{1.5-} ligands and is predicted to be a trivalent 4f¹ π^3 compound. Moreover, the multiconfiguration calculation points out that cerocene is described by the mixture of Ce(IV) (20%) and Ce(III) (80%) that results in the ¹A_{1g} ground state under D_{8h} symmetry. In our work, however, the photoelectron spectrum of Ce(C₈H₈)₂⁻ is strikingly similar to that of Nd(C₈H₈)₂⁻, which is calculated to be represented purely by Nd(III). From our work, the mixing of Ce(IV) cannot be recognized. The theoretical calculation on Ce(C₈H₈)₂ predicts that the excited state of ³E_{3g} should be 1.09 eV above the ground state.¹³ Correspondingly, band A is observed 1.06 eV above band X in Ce(C₈H₈)₂, and thus band A can be assigned to ³E_{3g}. For Nd-(C₈H₈)₂, the theoretical calculation predicts that the excited state of ⁵E_{3g} should be 0.18 eV above the ground state of ³E_{3g}.¹⁴ Since ³E_{3g} and ⁵E_{3g} are generated from the same electronic configuration, the band of ⁵E_{3g} should be five-thirds times more intense than that of ³E_{3g} due to the multiplicity of the electron spin, if the band is observable in this range. From the photoelectron spectrum, however, band ⁵E_{3g} could not be identified.

3.2.b. Photoelectron Spectra of Eu(C₈H₈)₂ and Yb(C₈H₈)₂. Eu and Yb are typical examples for stable Ln²⁺ complexes in bulk materials. This is because Eu and Yb possess 4f⁷ and 4f¹⁴ configurations in the oxidation states of +2, which corresponds to the half- and full-filled 4f orbitals, respectively, stabilized by the spin-spin exchange interaction. Therefore, their neutrals are considered to take Eu²⁺(C₈H₈)₂ and Yb²⁺(C₈H₈)₂ configurations. The difference in electronic and vibrational structures from Ln³⁺ complexes is ascribed to the change of electronic configuration of C₈H₈ from (C₈H₈)^{1.5-} to (C₈H₈)⁻. In the photoelectron spectra, two strong bands were observed and their gaps are 0.54 eV for neutral Eu(C₈H₈)₂ and 0.52 eV for neutral Yb(C₈H₈)₂. On the basis of the assignment for Ce(C₈H₈)₂⁻, Nd(C₈H₈)₂⁻, and Ho(C₈H₈)₂⁻, the two bands in Eu(C₈H₈)₂⁻ and Yb(C₈H₈)₂⁻ are assigned to those from e_{2u} and e_{2g}, respectively, although it seems that the neutral Eu-(C₈H₈)₂ and Yb(C₈H₈)₂ have lower symmetry than D_{8h} due to deformation of the eight-membered ring of C₈H₈. Furthermore, the apparent broadening of these bands with the heavier lanthanide atoms is noticeable. Since there is no unpaired f electron in Yb(C₈H₈)₂, the broadening might be attributed not to the exchange interaction with the f electrons, but to the vibrational excitations of the ligand C₈H₈. On the high-energy side of the electron-binding energy, broader bands were found 1 eV above band X, and they might be contributed from the oxidation states of +3; the photodetachment from Ln²⁺(C₈H₈)₂^{1.5-}

(26) See, e.g.: (a) Dewar, M. J. S.; Gleicher, G. J. *J. Am. Chem. Soc.* **1965**, *87*, 685. (b) Fray, G. I.; Saxton, R. G. *The Chemistry of Cyclooctatetraene and its Derivatives*. Cambridge University Press: Cambridge, 1978.

(27) Streitwieser, A., Jr.; Kinsley, S. A.; Rigsbee, J. T. *J. Am. Chem. Soc.* **1985**, *107*, 7786. In their report, although they commented on nothing around 4.8 eV in (He I) the photoelectron spectrum, there indeed exists one peak that can be assigned as 4f-originated ionization.

(28) Clark, J. P.; Green, J. C. *J. Chem. Soc., Dalton Trans.* **1977**, 505.

(29) These values were determined from the difference of VDEs of two peaks in the photoelectron spectrum at 266 nm.

(30) Perec, M. *Spectrochim. Acta* **1991**, *47A*, 799.

Table 2. Assignments of Electronic States of Anionic and Neutral Lanthanocenes and Multiplicity of Electron Spin ($2S + 1$)

species	state configuration	electronic states ^a	$2S + 1$
Ce(C ₈ H ₈) ₂ ⁻	4f ¹ π ⁴ ; Ce ³⁺ (C ₈ H ₈ ²⁻) ₂	² E _{2u}	2
Ce(C ₈ H ₈) ₂	4f ¹ π ³ ; Ce ³⁺ (C ₈ H ₈ ^{1.5-}) ₂	¹ A _{1g} ^b	1
Nd(C ₈ H ₈) ₂ ⁻	4f ³ π ⁴ ; Nd ³⁺ (C ₈ H ₈ ²⁻) ₂	E _{3g} × E _{2u} ^c	4
Nd(C ₈ H ₈) ₂	4f ³ π ³ ; Nd ³⁺ (C ₈ H ₈ ^{1.5-}) ₂	³ E _{3g} ^b	3
Ho(C ₈ H ₈) ₂ ⁻	4f ¹⁰ π ⁴ ; Ho ³⁺ (C ₈ H ₈ ²⁻) ₂		5
Ho(C ₈ H ₈) ₂	4f ¹⁰ π ³ ; Ho ³⁺ (C ₈ H ₈ ^{1.5-}) ₂		4 or 6
Eu(C ₈ H ₈) ₂ ⁻	4f ⁷ π ³ ; Eu ²⁺ (C ₈ H ₈ ^{1.5-}) ₂		7 or 9
Eu(C ₈ H ₈) ₂	4f ⁷ π ² ; Eu ²⁺ (C ₈ H ₈ ¹⁻) ₂		8 or 10
Yb(C ₈ H ₈) ₂ ⁻	4f ¹⁴ π ³ ; Yb ²⁺ (C ₈ H ₈ ^{1.5-}) ₂	² E _{2u}	2
Yb(C ₈ H ₈) ₂	4f ¹⁴ π ² ; Yb ²⁺ (C ₈ H ₈ ¹⁻) ₂	E _{2u} × E _{2u}	1 or 3

^a Symmetry under D_{8h}. ^b Calculation in ref 14. ^c One of the products should be assigned.

to Ln³⁺(C₈H₈^{1.5-})₂. In Table 2, the most probable assignments for the electronic configuration of anionic (1, 2)⁻ and neutral (1, 2) are tabulated, including the multiplicity of electron spin. Since the stability of Eu²⁺ is ascribed to the half-filled 4f orbitals, Eu(C₈H₈)₂ should evidently have the high multiplicity of electron spin. Although it is difficult to define the symmetry of the ground state at the present stage, the high electron spin should result in the high value of the total angular momentum *J*, which directly offers a magnetic moment of the complex through the large spin-orbit coupling. The magnetic properties of Eu-C₈H₈ and other Ln-C₈H₈ complexes will also give invaluable information on the physics of the organolanthanide for the future.

As pointed out in this section, larger anions having the composition of (n, n + 1)⁻ (n ≥ 2) were efficiently produced only for Eu_n(C₈H₈)_{n+1}⁻ and Yb_n(C₈H₈)_{n+1}⁻. This can be explained by the charge distributions in the complexes. For the (1, 2)⁻ anion, one more electron is acceptable in Ln²⁺[(C₈H₈)^{1.5-}]₂ having the oxidation state of +2 because two C₈H₈ molecules can absorb up to four electrons. Then, the acceptability seemingly enables the (1, 2)⁻ anion to grow into larger complexes with the ionic bond formation. On the other hand, the (1, 2)⁻ anion having the oxidation state of +3, Ln³⁺[(C₈H₈)²⁻]₂, becomes so stable by itself that no larger complexes are produced.

3.3. Ionization Energies of Neutral Ln_n(C₈H₈)_{n+1} Complexes. For neutral and cationic Ln-C₈H₈ complexes, larger complexes having (n, n + 1) compositions were successfully produced as shown in Figure 1. To know the electronic properties the ionization energies (E_is) of the neutral Ln_n(C₈H₈)_n were measured by using photoionization spectroscopy.

Figure 4 shows a typical example of the photoionization efficiency (PIE) curves for Nd_n(C₈H₈)_{n+1} for n = 1–3. Their E_is were determined from the final decline of the curve: 5.06, 5.02, and 4.15 eV for n = 1–3, respectively. Similarly, the E_is of the other Ln_n(C₈H₈)_{n+1} were measured and tabulated in Table 3. In the table, the lower and the upper limits of E_is for Eu and Yb complexes are also listed. These complexes cannot be photoionized by 5.92 eV photons, but can be ionized by 6.42 eV photons of the ArF laser, where the energy of 5.92 eV corresponds to the limit of the tunable range of the UV laser. For Ce, only E_i of (1, 2) was measured due to the poor intensity of larger complexes.

When the size dependence of E_i is shown as Figure 5, two patterns are easily conceivable. For Nd_n(C₈H₈)_{n+1} and Ho_n(C₈H₈)_{n+1} (Figure 5a), while E_is of (1, 2) and (2, 3) show similar values, E_is of (3, 4) largely drop by 0.8 eV. For Eu_n(C₈H₈)_{n+1} and Yb_n(C₈H₈)_{n+1} (Figure 5b), however, the E_i values are almost

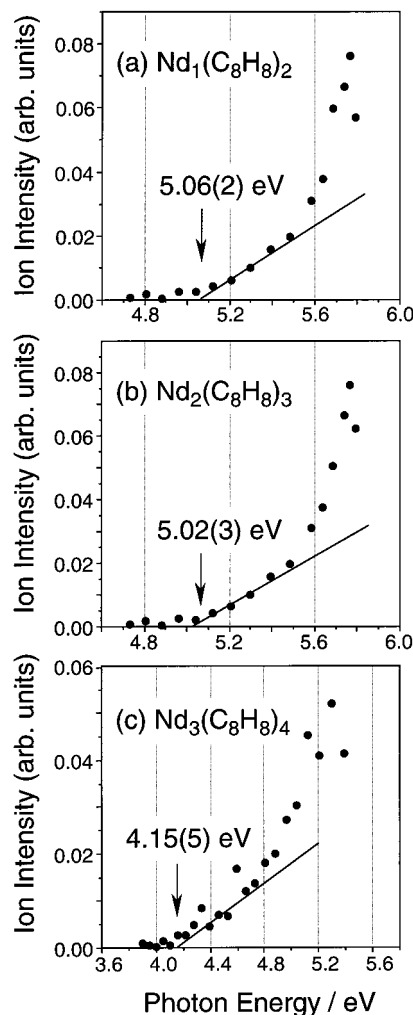


Figure 4. Typical example of photoionization efficiency (PIE) curves for Nd_n(C₈H₈)_{n+1} for n = 1–3. Their E_is were determined from the final decline of the curve: 5.06, 5.02, and 4.15 eV for n = 1–3, respectively. The E_i of (3, 4) drops drastically by 0.8 eV.

Table 3. Ionization Energies (E_is) of the Sandwich Ln_n(C₈H₈)_{n+1} (n = 1–3) (eV)

Ln element	n	E _i ^a	
Ce	1	5.27(5)	
Nd	1	5.06(2)	
	2	5.02(3)	
	3	4.15(5)	
Eu	1, 2, 3	5.92 < E _i < 6.42	
	Ho	1, 2	5.92 < E _i < 6.42
		3	5.35(8)
Yb	1, 2	5.92 < E _i < 6.42	
	3	5.89 < E _i < 6.42	

^a Numbers in parentheses indicate experimental uncertainties; 5.27(5) represents 5.27 ± 0.05. “5.92 < E_i < 6.42” represents that lower and upper limits are 5.92 and 6.42 eV, respectively. 5.92 eV corresponds to the highest energy of the second harmonics of the dye laser, and 6.42 eV corresponds to the energy of the ArF laser.

constant for n = 1–3, although the values have relatively large uncertainty. The two size dependences can be explained by the counting of valence electrons, based on the multiple ionic states in the complex. Considering that Ln atoms favor the Ln³⁺ or Ln²⁺ state in the ligand field, allotment of valence electrons in multiple decker Ln_n(C₈H₈)_{n+1} should be attributed as shown in Figure 6. In case of Nd and Ho, Ln atoms can exist as Ln³⁺ ions interposed by C₈H₈ for n = 1 and 2. For n = 3, however, one of the Ln atoms in the multiple-decker structure cannot

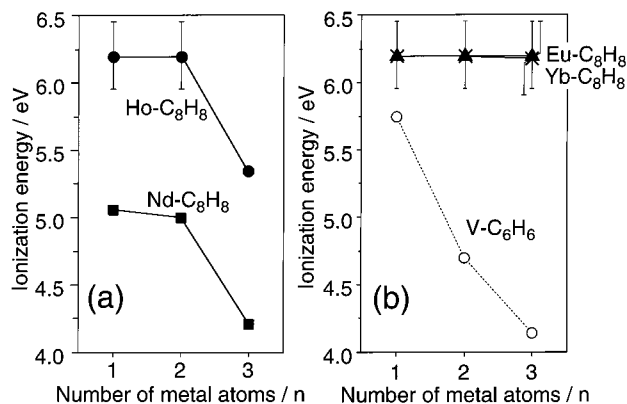


Figure 5. Ionization energies (E_{iS}) of multiple decker sandwich complexes: (a) $Nd_n(C_8H_8)_{n+1}$ (solid square) and $Ho_n(C_8H_8)_{n+1}$ (solid circle); (b) $Eu_n(C_8H_8)_{n+1}$ (solid triangle), $Yb_n(C_8H_8)_{n+1}$ (cross lines), and $V_n(C_6H_6)_{n+1}$ (open circle). E_{iS} of $V_n(C_6H_6)_{n+1}$ complexes were referred from ref 22.

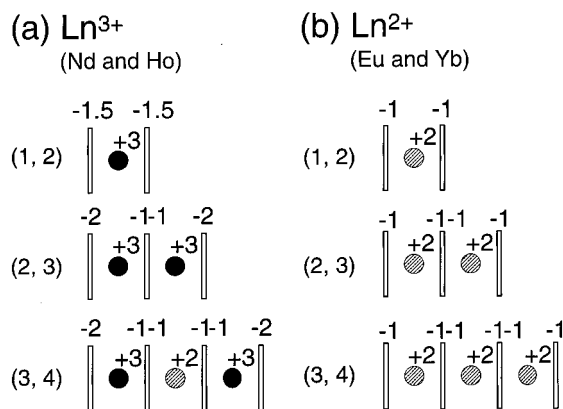


Figure 6. Allotment of valence electrons of $Ln_n(C_8H_8)_{n+1}$ complexes: (a) $Ln = Nd$ and Ho ; (b) $Ln = Eu$ and Yb . These schematics are based on the assumption of the 2-electrons acceptability of C_8H_8 and multiply charged positive ions of Ln (Ln^{3+} for Nd and Ho , and Ln^{2+} for Eu and Yb). As shown in (a), one of the Ln atoms should become the +2 oxidation state in (3, 4).

become the Ln^{3+} ion because of the lack of electron acceptability in C_8H_8 . Then the central Ln atom should result in a Ln^{2+} ion. Especially for Eu and Yb , complexes can grow up keeping the Ln^{2+} ion, as shown in Figure 6b. When we look at the tendency of E_{iS} , drops of E_{iS} at $Ln_3(C_8H_8)_4$ ($Ln = Nd$ and Ho) can be reasonably explained by the change of valence electrons as follows: Since the central Ln atom in (3, 4) should take the Ln^{2+} ion in the neutral, large stabilization is expected for the cationic (3, 4)⁺ by changing the charge from Ln^{2+} to Ln^{3+} . In (1, 2) and (2, 3), on the other hand, no cationic stability is expected because the ionization process results in the change from Ln^{3+} to Ln^{4+} .

In a larger sandwich complex ($n \geq 3$), therefore, the oxidation state always becomes +2 for the Ln atoms around the core of the neutral complex, while terminal Ln atoms in both ends are +3. It is well-known that some of the Ln atoms, notably Tb , Ho , and Eu , show characteristic strong emission bands from the visible to the ultraviolet region, and the energies and intensities depend on the oxidation states of +2 and +3. Then, the mixing of the different oxidation states in the complex seemingly leads to the combination of optical properties.

For all of the Eu and Yb complexes, Eu and Yb atoms always take Ln^{2+} in the neutrals as shown in Figure 6b. Rather high E_{iS} of $Eu_n(C_8H_8)_{n+1}$ compared to the Eu atom are ascribed to the stability of neutral complexes, in which central Eu^{2+} has

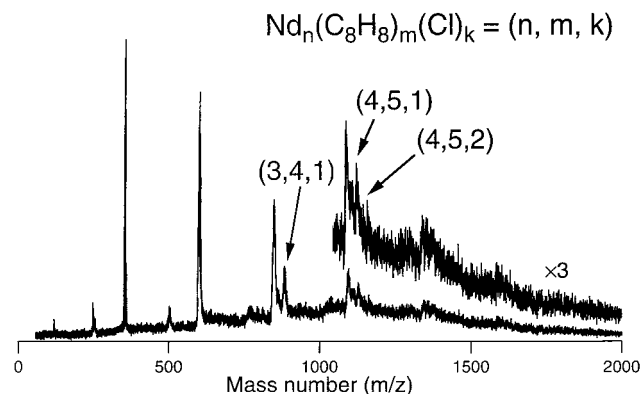


Figure 7. Typical example of the mass spectrum of $Ln_n(C_8H_8)_m$ ($Ln = Nd$) complexes after the reaction of CCl_4 gas. While compositions of (1, 2) and (2, 3) showed no reaction, (3, 4) and (4, 5) produced (3, 4) + Cl and a small amount of (4, 5) + $Cl_{1,2}$ adducts, respectively, which further supports the charge distribution in the multiple decker $Ln_n(C_8H_8)_{n+1}$. See text.

the $4f^7$ half-closed shell configuration. Since the Nd atom ($4f^3$) in the complex is an open shell configuration in neutral, E_{iS} of $Nd_n(C_8H_8)_{n+1}$ showed low E_{iS} compared to the Nd atom ($E_{i-}[Nd] = 5.49$ eV). Rather high E_{iS} for the $Ho_n(C_8H_8)_{n+1}$ compared to $Nd_n(C_8H_8)_{n+1}$ might be ascribed to the higher E_i of Ho atom (6.02 eV) than that of the Nd atom (5.49 eV).

In the previous report on multiple-decker sandwiches of $V_n(C_6H_6)_{n+1}$ ($n = 1-4$),²² E_{iS} showed a drastic decrease as the complex size increased. This phenomenon of E_i is theoretically attributed³¹ to the ionization occurring from the delocalized molecular orbital of vanadium–vanadium interaction interposed by π^* orbitals of benzene. In $Ln_n(C_8H_8)_{n+1}$, however, an orbital contributing to the ionization process is considered to be discontinuously localized along the molecular axis, because the complex is bonded through ionic bonds and the charge is localized at each component. Since the first ionization is expected to occur from $4f(Ln)$ orbitals in (1, 2),^{27,28} we concluded that the $4f$ orbital in the complex is localized and scarcely interacts with neighboring Ln atoms in the complex. According to the theoretical calculation of Dolg and co-workers,¹⁴ $Nd(C_8H_8)_2$ is a charge-transfer complex in which 3 of 6 electrons in $Nd(6s^2 4f^4)$ transfer almost completely to $2C_8H_8$, resulting in a configuration of $Nd^{3+}(C_8H_8^{1.5-})_2$. In case of Eu and Yb , although we are unaware of the extent of the charge transfer in the complexes, rather high E_{iS} of $Eu_n(C_8H_8)_{n+1}$ and $Yb_n(C_8H_8)_{n+1}$ seem to ensure the complete charge transfer, because E_{iS} of Eu and Yb complexes are rather high (5.92 eV < E_{iS} < 6.42 eV) compared to those of Ln^{3+} complexes. We conclude from all the results that bonding in $Ln_n(C_8H_8)_{n+1}$ is ionic, in which Ln atoms exist as Ln^{3+} or Ln^{2+} ions. Moreover, the multiply ionic character for the $Ln-C_8H_8$ complexes strongly suggests that the binding energy between the Ln atoms and the ligand molecules is much stronger than that of the $V-C_6H_6$ complex, which was estimated to be 1–2 eV.

The result of the chemical reaction with CCl_4 gas with the second FTR mounted downstream of the C_8H_8 addition port deserves comment. A typical example of the mass spectrum on Nd is shown in Figure 7. While compositions of (1, 2) and (2, 3) showed no reaction toward CCl_4 , (3, 4) and (4, 5) produced the adducts of (3, 4) + Cl and a small amount of (4, 5) + $Cl_{1,2}$, respectively. Generation of the $Nd_3(C_8H_8)_4Cl$ adduct is reasonably attributed to the electronic structure of $C_8H_8^{2-}$ —

(31) Yasuike, T.; Yabushita, S. *J. Phys. Chem. A*. Submitted for publication.

$\text{Nd}^{3+}-\text{C}_8\text{H}_8^{2-}-\text{Nd}^{2+}-\text{C}_8\text{H}_8^{2-}-\text{Nd}^{3+}-\text{C}_8\text{H}_8^{2-}$, because the attack of the Cl atom on the complex leads to $\text{Nd}_3^{3+}(\text{C}_8\text{H}_8^{2-})_4\text{Cl}^-$ through the dissociative electron attachment of CCl_4 that gives CCl_3 and Cl^- . Although the utmost number of $\text{Nd}_4(\text{C}_8\text{H}_8)_5$ adducts is indistinguishable in this experiment, the adduct of $\text{Nd}_4(\text{C}_8\text{H}_8)_5\text{Cl}_2$ probably corresponds to the configuration of $(\text{Nd}^{3+})_4(\text{C}_8\text{H}_8^{2-})_5(\text{Cl}^-)_2$. This result for formation of halogen atom adducts also suggests the charge distribution in $\text{Nd}_n(\text{C}_8\text{H}_8)_{n+1}$ as shown in Figure 6a.

4. Conclusions

$\text{Ln}_n(\text{C}_8\text{H}_8)_{n+1}$ ($\text{Ln} = \text{Nd}, \text{Eu}, \text{Ho}, \text{and Yb}$) were produced by the combination of the laser vaporization and the molecular beam method in the gas phase. The conclusions obtained are as follows: (1) These complexes are multiple-decker sandwich structures in which Ln atoms and C_8H_8 molecules are alternately stacked. (2) Further, $\text{Ln}_n(\text{C}_8\text{H}_8)_{n+1}$ are charge-transfer complexes, where the Ln atoms are multiply charged cations of Ln^{k+} ($k = 2$ and 3) and C_8H_8 molecules are multiply charged anions of $\text{C}_8\text{H}_8^{h-}$ ($h = 1, 1.5, \text{and } 2$). (3) $4f$ orbitals of Ln atoms in $\text{Ln}_n(\text{C}_8\text{H}_8)_{n+1}$ are localized on the metal atom. As demonstrated

in many areas of modern technology, the unusual properties of the lanthanide elements widely play an important role in catalytic, optical, and magnetic materials. Then, the gas-phase preparation of the novel structure of the organolanthanide complexes should open up a new area of development for the advanced materials. A large-scale deposition of the size-selected organolanthanide complexes enables us to examine and to characterize the optical, magnetic, and catalytic properties of these sandwich complexes in detail. The deposition experiment of the $\text{Ln}-\text{C}_8\text{H}_8$ complex is actively in progress in our group.

Acknowledgment. This work is supported by a program entitled "Research for the Future (RFTF)" of Japan Society for the Promotion of Science (98P01203) and by a Grant-in-Aid for Scientific Research on Priority Areas from the Ministry of Education, Science, Sports, and Culture. A.N. expresses his gratitude to the Morino foundation for molecular science for partial financial support. T.K. expresses his gratitude to Research Fellowships of the Japan Society for the Promotion of Science for Young Scientists.

JA982438T